7-2002

Oceanographic Observations in Chilean Coastal Waters Between Valdivia and Concepcion

Larry P. Atkinson
Old Dominion University, atkinso@odu.edu

Arnoldo Valle-Levinson
Old Dominion University

Dante Figueroa

Ricardo De Pol-Holz

Victor A. Gallardo

See next page for additional authors

Original Publication Citation

Atkinson, L. P., Valle-Levinson, A., Figueroa, D., De Pol-Holz, R., Gallardo, V. A., Schneider, W., . . . Schmidt, M. (2002). Oceanographic observations in Chilean coastal waters between Valdivia and Concepcion. *Journal of Geophysical Research-Oceans, 107*(C7, 3081), [1-14]. doi: 10.1029/2001jc000991

Authors
Larry P. Atkinson, Arnoldo Valle-Levinson, Dante Figueroa, Ricardo De Pol-Holz, Victor A. Gallardo, Wolfgang Schneider, Jose L. Blanco, and Mike Schmidt

Oceanographic observations in Chilean coastal waters between Valdivia and Concepción

Larry P. Atkinson,[1] Arnoldo Valle-Levinson,[1] Dante Figueroa,[2] Ricardo De Pol-Holz,[2] Victor A. Gallardo,[2] Wolfgang Schneider,[2] Jose L. Blanco,[1] and Mike Schmidt[3]

Received 23 May 2001; revised 29 November 2001; accepted 11 December 2001; published 25 July 2002.

[1] The physical oceanography of the biologically productive coastal waters of central Chile (36° to 40°S) is relatively unknown. In December 1998 we made a short exploratory cruise between Valdivia (40°S) and Concepción (37.8°S) taking temperature, salinity, oxygen, and current velocity profiles. Coincident sea surface temperature and color measurements were obtained by satellite. The results showed an area dominated by wind-induced coastal upwelling, river runoff, intrusion of offshore eddies, mixing, and heating. Upwelling centers were found over the shelf at three locations: inshore of Mocha Island, off Valdivia, and off Lavapie Point. At these centers, equatorial subsurface water (ESSW) intrudes into the coastal waters, sometimes affecting the surface waters. Since ESSW has characteristically low-oxygen and high-salinity values, it is easily detected. Off Valdivia, runoff imparts stratification, while farther north, solar heating and reduced mixing may facilitate stratification. In some areas, even strong winds would not destroy the stratification imparted by the advection of buoyancy that occurs during the upwelling process. Strong equatorward currents (>1 m s^{-1}) in the form of an upwelling jet were found off Lavapie Point. This is also the location of an intruding anticyclone. Elsewhere, currents were mainly northward but highly variable because of intrusions from offshore eddies. The sea surface temperature and ocean color images show a complex field of onshore and offshore intrusions combined with the effects of mixing on chlorophyll concentrations. The residence time of upwelled water on the shelf is estimated to be less than 1 week. *INDEX TERMS:* 4279 Oceanography: General: Upwelling and convergences; 4516 Oceanography: Physical: Eastern boundary currents; 4528 Oceanography: Physical: Fronts and jets; *KEYWORDS:* Upwelling; wind; water circulation; eddies; central Chile coast

1. Introduction

[2] The coastal waters of Chile are unique because a combination of meteorological and oceanographic processes and geography has created one of the world's most biologically productive ocean areas. The coast extends in a nearly north/south direction over 40° of latitude (not including the Antarctic) bordered by the Andes to the east and the Peru-Chile Trench to the west. Thus Chilean coastal waters lie between two of the highest relief features on Earth. Over this vast latitudinal range, climatic conditions vary from arid to subantarctic with upwelling winds off northern Chile, downwelling winds off southern Chile, and strong westerlies and considerable variability between. Rainfall toward the north is in some places nonexistent, while farther south it is quite high. The extremely high productivity of the Chilean coastal waters is attributable to upwelling of nutrient rich Peru-Chile Undercurrent water [*Strub et al.*, 1998] and processes that maintain biological populations in the shallow coastal waters.

[3] In December 1998 we made an exploratory cruise along the coast between Valdivia (40°S) and Concepción (37.8°S). This region is noted for its extremely high biological productivity that sometimes provides 4% of the world's fish catch. Our preliminary results, based on a unique but sparse data set, show the structure of currents, upwelling centers, and low-salinity water along the coast and the relationship to satellite-derived SST and chlorophyll.

2. Regional Setting

[4] The region studied has a broad shelf that gradually narrows to the north at Lavapie Point (Figure 1). The shelf is about 50 km wide south of Tucapel Point with Mocha Island lying on the outer shelf marking the widest and shallowest part of the shelf. North of Tucapel Point the shelf narrows to about 10 km then starts to widen again at Lavapie Point. The broad and shallow Gulf of Arauco lies northeast of Lavapie Point. The Gulf of Arauco is a large embayment with Santa Maria Island lying offshore inline with the coast to the south. The Bio Bio River flows into the northern end of the Gulf, and the submarine canyon

[1]Old Dominion University, Norfolk, Virginia, USA.
[2]University of Concepción, Concepción, Chile.
[3]Goddard Space Flight Center, NASA, Greenbelt, Maryland, USA.

0148-0227/02/2001JC000991

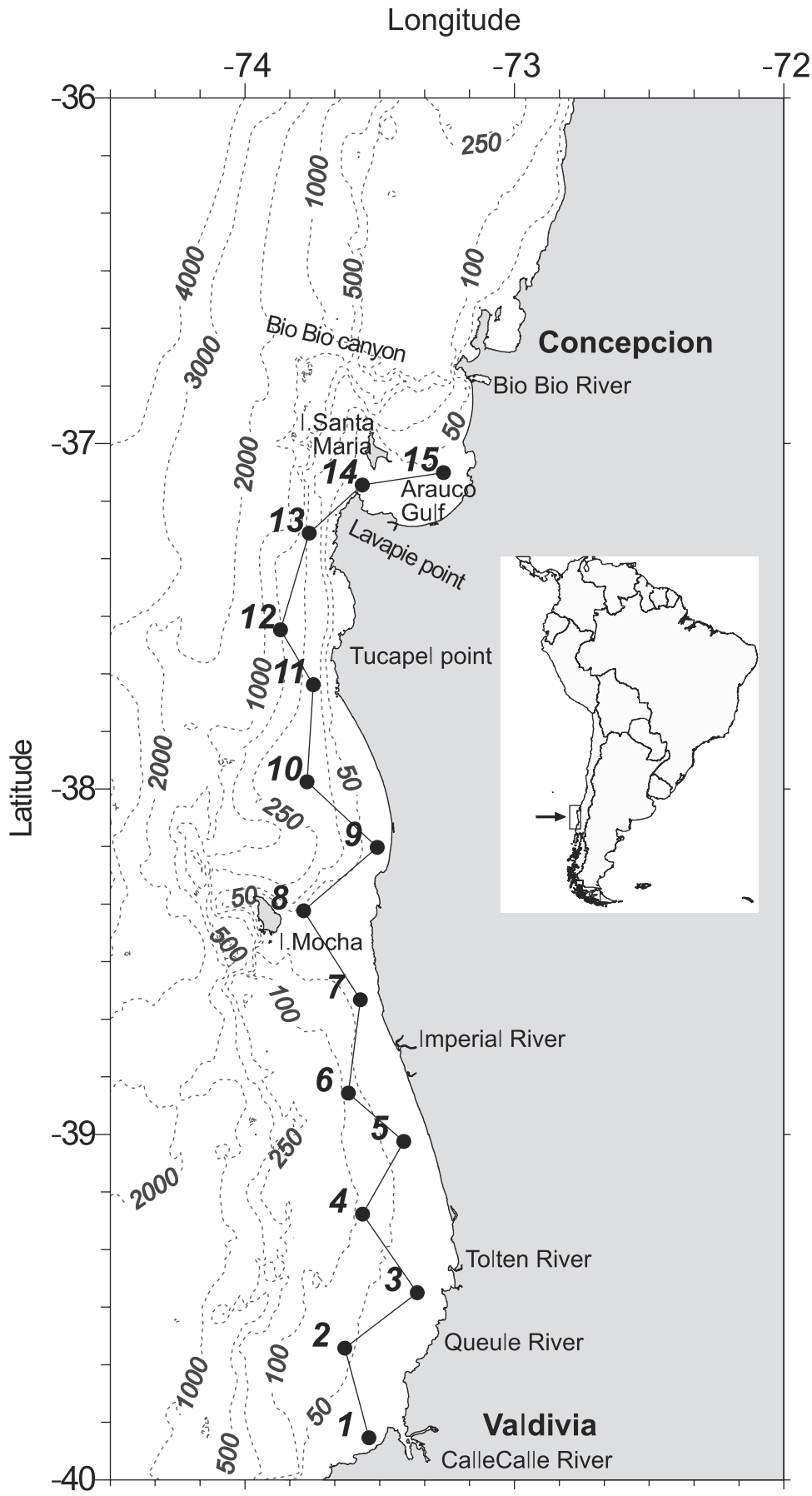
Longitude
-74
-73
-72
-36
-37
-38
-39
-40
Latitude
250
1000
4000
500
100
3000
Bio Bio canyon
Concepcion
Bio Bio River
I.Santa
Maria
50
2000
14
15
Arauco
Gulf
13
Lavapie point
12
Tucapel point
11
1000
2000
10
50
250
9
50
8
I.Mocha
500
7
100
Imperial River
6
5
250
2000
4
Tolten River
3
2
Queule River
1000
100
50
1
Valdivia
500
CalleCalle River

associated with the Bio Bio River crosses the shelf west of its present mouth.

[5] It is important to note two geographic features that affect the wind field. The first feature is change in coastline direction at Lavapie Point. South of Lavapie Point the coastline trends toward 355°T, while north of Lavapie Point the shore trends toward 20°T. The Gulf of Arauco itself represents a large-scale equatorward facing embayment in the 20°T trending coast. Response to upwelling winds depends on the changing trends of the general bathymetry that follows the shoreline. The changing shoreline direction and diverging isobaths at Lavapie Point would induce upwelling in a northward flowing current [*Arthur*, 1965; *Blanton et al.*, 1981].

[6] The coastal wind field may also be affected by the presence of a coastal range of mountains extending from Concepción southward to the latitude of Mocha Island: the Cordillera de Nahuelbuta. North and south of the Cordillera de Nahuelbuta the coastal range is relatively low in relief. However, maximum heights in the range reach over 1000 m. These heights may cause intensified winds in the adjacent coastal waters.

[7] River flow into the region consists of the Bio Bio River (36.8°S) to the north and the Imperial River (38.8°S), Tolten River (39.2°S), Queule River (39.6°S), and the Calle Calle River (39.8°S) to the south. The previously mentioned cordillera blocks westward flowing rivers in the central part of the region. The total flow in the region from 37° to 40°S is about 3100 $m^3\ s^{-1}$ or 100 $km^3\ yr^{-1}$ [*Davila et al.*, 2000]. This amount of flow is not large but would be expected to produce areas of low salinity and coastal currents for a few tens of kilometers around the river mouths during the rainy winter season and early summer when the snow melts. South of 40°S the river flow increases significantly relative to flow to the north.

[8] The water mass and general circulation characteristics off central Chile were recently summarized [*Strub et al.*, 1998], so we will keep the review here to a minimum. Wind-driven coastal upwelling is the dominant process in the area during the summer. The cold, salty, nutrient-rich, oxygen-poor equatorial subsurface water (ESSW) flowing southward in the Peru-Chile Undercurrent upwells across the shelf and often intrudes to the coast [*Gunther*, 1936; *Silva and Neshyba*, 1979].

[9] Satellite-derived sea surface temperature imagery [*Cáceres*, 1992] shows filaments and offshore eddies in the region. Offshore anticyclonic eddies are most often found north of Lavapie Point. Offshore-flowing filaments are concentrated in the region just north of Mocha Island and off the Gulf of Arauco. Our data show that offshore and onshore flow affects the inshore waters that we sampled.

3. Methods

[10] In this section we review the methods used and sources of data. The observations were made from the R/V *Kay Kay* operated by the Universidad de Concepción. Between 8 and 11 December 1998 the ship was taken along a path up the coast in a pattern dictated by the schedule and weather (Figure 1). Courses were laid out to sample the coastal current, upwelling centers, and other features of the region. Along the route, continuous current profiles were made with acoustic Doppler current profiler (ADCP) and conductivity-temperature-depth (CTD) casts were made at the end points of each zigzag leg.

[11] Mean monthly upwelling winds were obtained from the NOAA Pacific Fisheries Environmental Laboratory in Monterey, California. We used data from the 36°S node. Coastal winds were obtained from a station at Lavapie Point maintained by the Department of Physics of the Atmosphere and Ocean at the University of Concepción. There are no other wind observations in the region's coastal waters for this time period. Sea surface temperature data were from advanced very high resolution radiometer for 9 December 1998. Images for 10 and 11 December were contaminated with clouds but suggested surface warming consistent with the decreasing upwelling wind speeds. A SeaWifs image from 9 December 1998 was processed using the most recent algorithms for coastal waters.

[12] An RD Instruments Workhorse (300 kHz) ADCP was used to make the current velocity profiles. The ADCP was mounted on a 1.2-m-long catamaran towed several meters to the side of the ship. Raw data were averaged over 90 s and 1-m bins. Bottom tracking was always on, and navigation was by GPS. The data were not detided as the onshore offshore cruise track created nodes similar to tidal nodes if any were present. This was the first time an ADCP was used in this region of Chile.

[13] Temperature, oxygen and salinity profiles were made with a SeaBird 19 CTD. All data where processed using SeaBird software.

4. Results

[14] In this section the results of the observations and other ancillary data are described. First the winds and remotely sensed data are presented, followed by the subsurface observations.

[15] The mean monthly upwelling index (Figure 2a) was very high in late 1998 relative to other years. The short-term record (Figure 2b) shows that the upwelling during the year started in July 1998 and had reached very high values by December. It is clear that our sampling took place during a period of steadily increasing upwelling on the monthly scale. Data from Lavapie Point (Figure 3) indicate a pulse of strong upwelling winds late on 9 December then two smaller events on 10–11 December. The consistent wind stresses over 0.1 N m^{-2} no doubt led to the upwelling we observed, and the decreasing stress on the 10 and 11 December would have caused a decrease in wind-induced upwelling. It should be noted that the cruise was toward the end of an El Niño period and at the beginning of a La Niña.

[16] Coastal upwelling, as indicated by low surface ocean temperatures, was present throughout the region (Figure 4a). Lowest temperatures (10–11°C) were found in the upwelling centers. High temperatures (14–15°C) were observed in

Figure 1. (opposite) Geography of region showing coast, rivers, and bathymetry. Acoustic Doppler current profiler cruise track (solid line) and conductivity-temperature-depth (CTD) stations (1–15) are indicated.

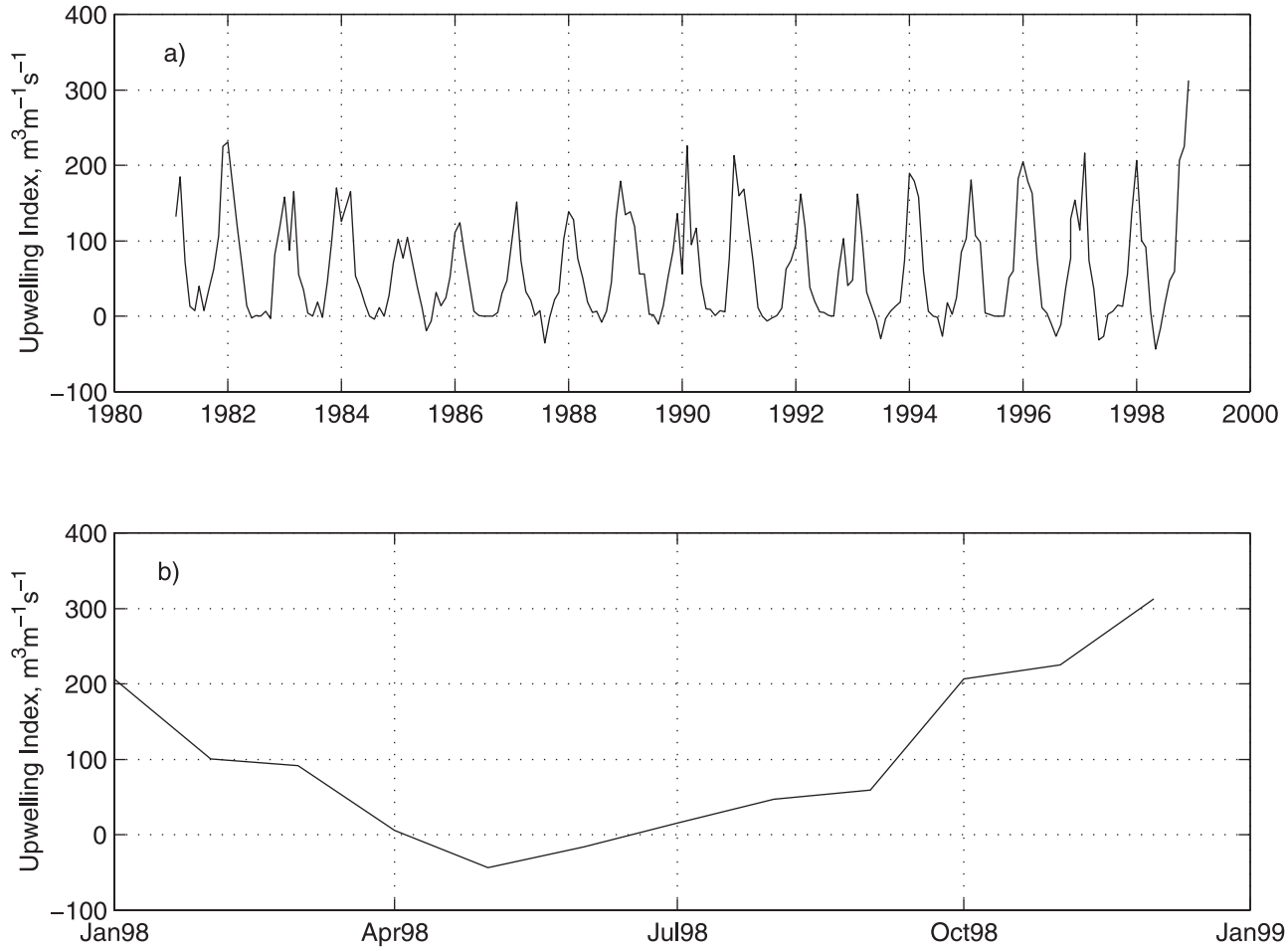

Figure 2. Interannual and monthly upwelling index at 36°S. (a) January 1981 to December 1999 and (b) January to December 1998.

some nearshore waters and in the offshore eddies. The upwelling pattern was, however, far from uniform. Each of these features (upwelling centers, onshore intrusions, and filaments) is described below.

[17] Areas of low SST were observed over the midshelf between 39° and 40°S with the low SST extending to the coast off Valdivia at 40°S. A second area of low SST was observed from 38.6° to 37.6°S over the shallow waters inshore of Mocha Island. The third area of low SST was in the expanding band of cold water north of Lavapie Point (37.6°S). As noted, this may be one continuous line of upwelling separated by the onshore flow from eddies or runoff plumes.

[18] In four locations, onshore intrusions of warm offshore water were observed. Those were south of 39.9° below Valdivia, around 39°, at 37.7°S off Tucapel Point, and off Lavapie Point. In some cases the warm intrusion placed 13°C or warmer water on the coast. Off Lavapie Point, upwelling water of 11° or 12°C was positioned between the coast and the warm offshore water, creating a high thermal gradient.

[19] Between the onshore intrusions of warm offshore water, cold filaments were seen that apparently advected colder coastal water offshore.

[20] The regions of high surface temperatures near shore in the southern part of the region may indicate more effective surface heating caused by higher stratification. The high stratification could be caused by buoyancy inputs from nearby rivers.

[21] The 9 December 1998 SeaWifs image (Figure 4b) shows the complex surface chlorophyll field and, by implication, the very complex current and upwelling structures. In the southern part of the region, surface chlorophyll was very high in the inshore waters. This pattern may reflect river influence nearshore and upwelling farther offshore. Inshore of Mocha Island the surface chlorophyll pattern appears to follow the SST. There are two cold filaments extending offshore north of Mocha Island and an inshore intrusion of warm water between the filaments. At Tucapel Point (37.7°S), surface chlorophyll is consistent with the surface temperature pattern with colder waters being higher in chlorophyll and vice versa. The lowest chlorophyll values were found offshore of Tucapel Point. North of Tucapel Point, surface chlorophyll is elevated in a band along the offshore edge of the upwelling front. Farther north at Lavapie Point the upwelling increases with the change in coastline orientation. Surface chlorophyll, however, remains relatively low in the upwelling plume north of Santa Maria Island but becomes higher inshore of the upwelling plume in the Gulf of Arauco and farther north.

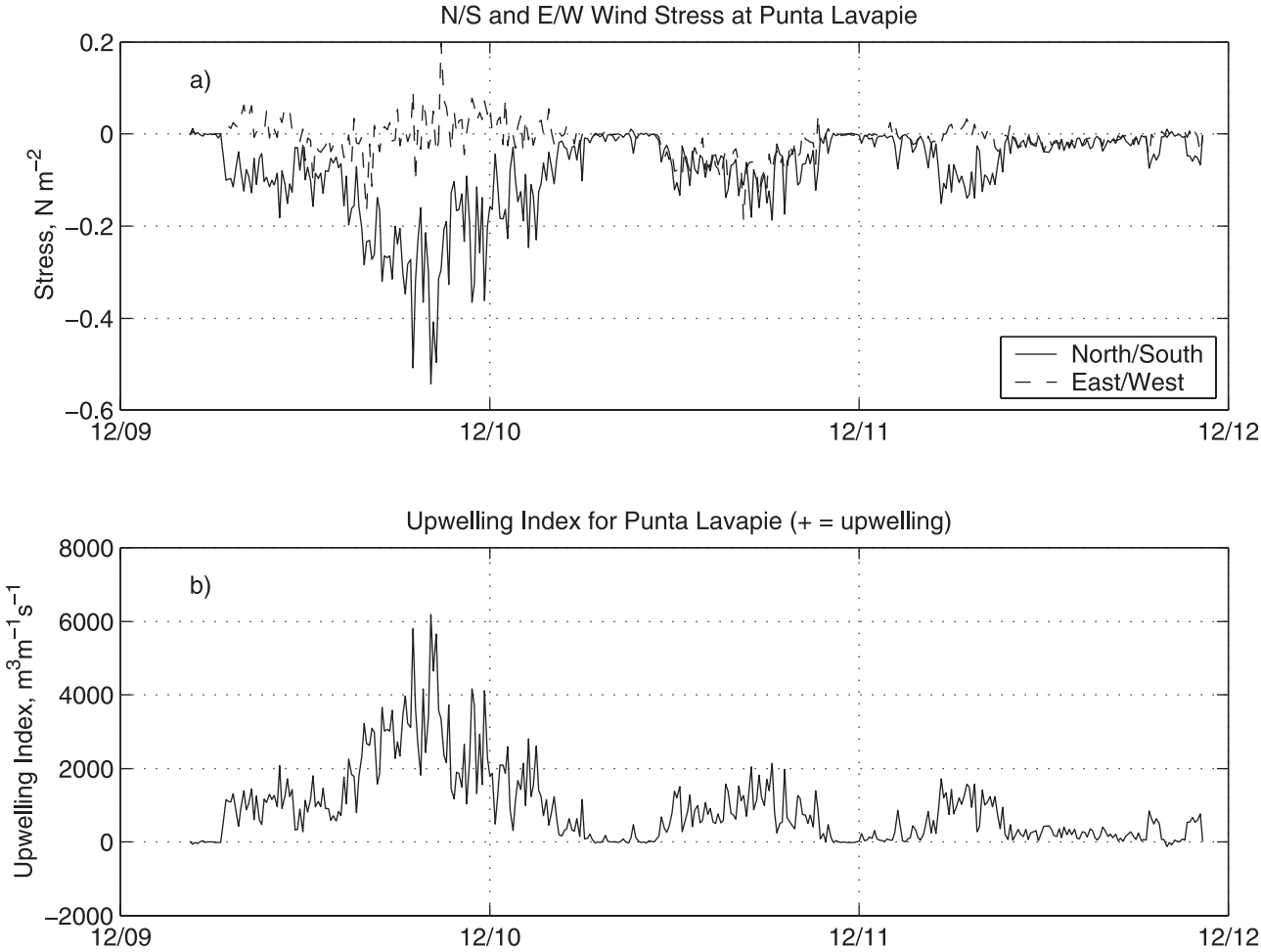

Figure 3. Lavapie Point hourly wind, 9–11 December 1998. (a) Wind stress and (b) upwelling index.

[22] The offshore filaments, both warm and cold, north of Arauco appear to be correlated with the surface chlorophyll: The offshore moving filaments have high chlorophyll, while the inshore flowing filaments have low chlorophyll.

[23] The current vectors from 4 m depth were overlaid on the 9 December SST image and SeaWifs images to aid in interpretation (Figure 4). Surface currents, in general, are consistent with dynamics inferred from the SST. The upwelling front north of 37.3°S features high northward currents (>1 m s^{-1}). In the vicinity of the shallow shelf inshore of Mocha Island, currents were flowing around a warm intrusion centered at 38.1°S. South of Mocha Island, currents were stronger toward the north in the upwelling front. Farther south (38.6°S), where the upwelling front seems less intense, currents are also weaker and mostly offshore. A warm onshore intrusion appears at 39°S, and the currents seem to flow around it as would be expected. Farther south to Valdivia, currents are more erratic, possibly reflecting the more incoherent SST patterns. Buoyancy-driven coastal currents were possibly present at 39.0°S and 39.4°S.

[24] Vertical sections of alongshore and across-shore currents (Figure 5) show the structure of the currents. Most noticeable is the northward jet off Lavapie Point (37.3°S; top right frame). The current is seen as being about 30 km wide and 20 to 60 m deep. Simple calculations suggest a flow between 0.5 and 1 Sv. Farther south, alongshore currents were less extensive; however, a northward flowing feature appeared in all transects. In each case the region of higher flow seemed to coincide with the boundary between the warmer offshore waters and cooler nearshore water. Regions of southward flow usually occurred in the deeper waters (> 20 m) and in the boundary between warmer nearshore water between 39.2°S and 38.7°S. Deeper alongshore flow was generally southward, reaching 0.2 m s^{-1}.

[25] Strongest onshore flow (Figure 5, left panels) occurred off Lavapie Point as might be expected from the SST distribution. Another area of onshore flow occurred at 39.2°S in the northward flow found there. Cross-shore flow varied from −0.2 to +0.2 m s^{-1}.

[26] The temperature/salinity and temperature/O_2 plots (Figure 6) are shown to elucidate the water masses and nonconservative processes in the region. The temperature/salinity plot shows that the resident waters are typical of ESSW: salinity from 34.3 to 34.5. Lower salinity at stations 1, 3, and 5 suggests that there was some mixing with river waters at a few stations. The very low O_2 values at stations 6, 9, and 10 indicate they, and especially station 9, represent what may be nearly undiluted ESSW. The different O_2 concentrations at the same temperatures suggest that photo-

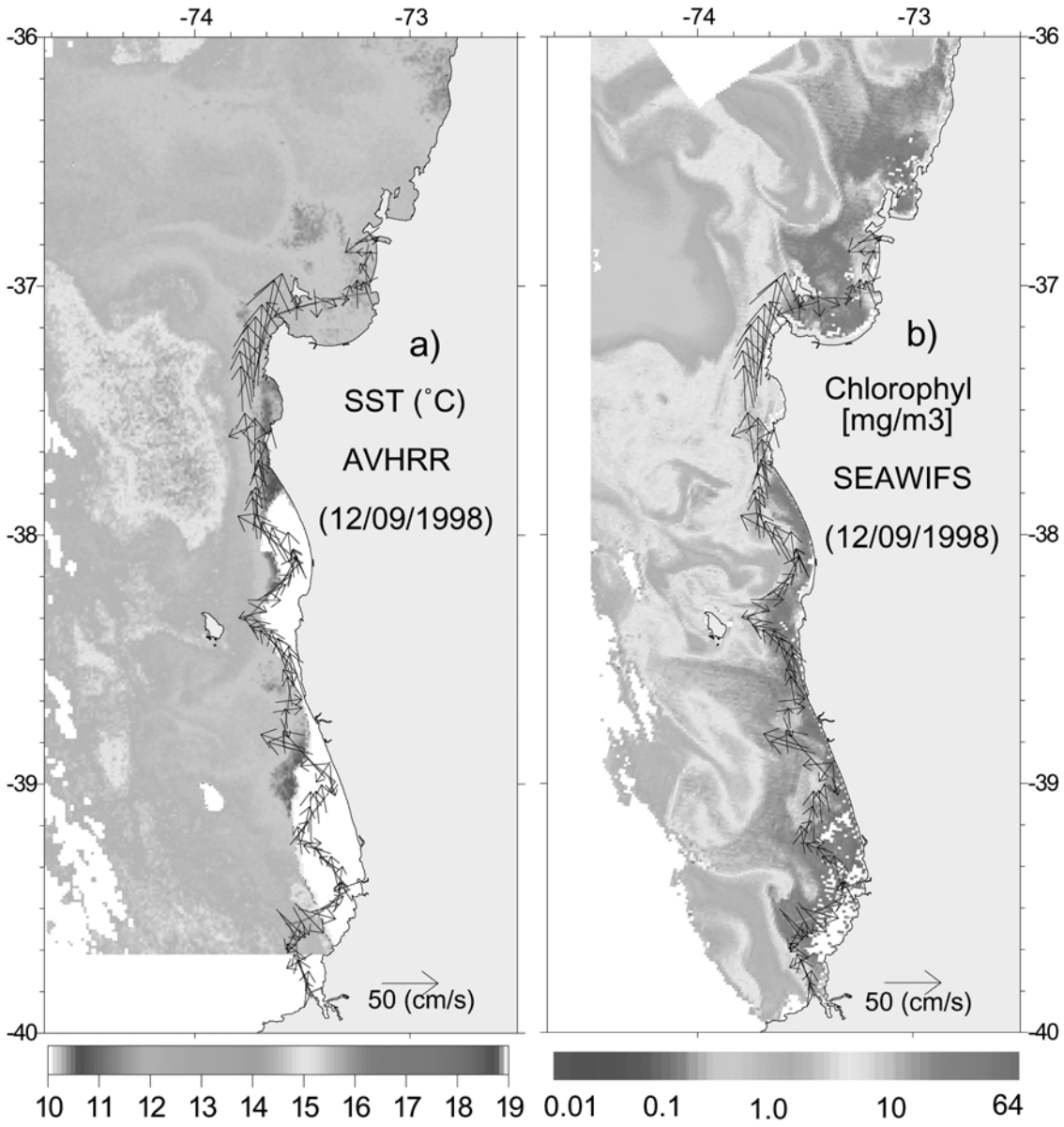

Figure 4. (a) Sea surface temperature from advanced very high resolution radiometer readings for 9 December 1998. (b) Surface chlorophyll SeaWifs image for 9 December 1998. Currents at 4 m depth, every fifth observation, are plotted. The 50 cm s^{-1} vector is indicated. See color version of this figure at back of this issue.

synthesis, oxidation processes, or warming changed the O_2 concentrations or solubility.

[27] The surface maps (Figure 7) were drawn using the data from the individual CTD profiles at stations. Surface temperatures (Figure 7a) follow very closely the distribution observed by satellite (Figure 4a) and show clearly the intrusion of warm offshore water around 39°S and cold-water areas with the minimum inshore of Mocha Island.

[28] The salinity results (Figure 7b) show a large area of lower salinity between Valdivia and the Imperial River. Highest salinity was coincident with the upwelling areas inshore of Mocha Island.

[29] Surface oxygen (Figure 7c) was higher around 39°S, coincident with the intrusion of warm water, and the minimum values are located in areas inshore of Mocha Island.

[30] Surface density (Figure 7d) is controlled by upwelling and runoff. Thus south of the Imperial River σ_t decreased to less than 25 alongshore, while inshore of Mocha island it was over 26. The baroclinic currents suggested by the density distribution are consistent with the ADCP observed currents north of 39.25°S. South of there, observed currents are weak or southward, inconsistent with the density field.

[31] Potential energy anomaly (Figure 7e) shows the water column stratification. Two areas with high values (>60 J m^{-3}) were found: One is in the south area (39.5°–40°S) related to the river inflow, and the other is related to the intrusion of warm and salty water offshore Lavapie Point.

[32] The thirteen profiles of temperature, salinity, and O_2 are shown in Figure 8. The strong thermocline is attributed

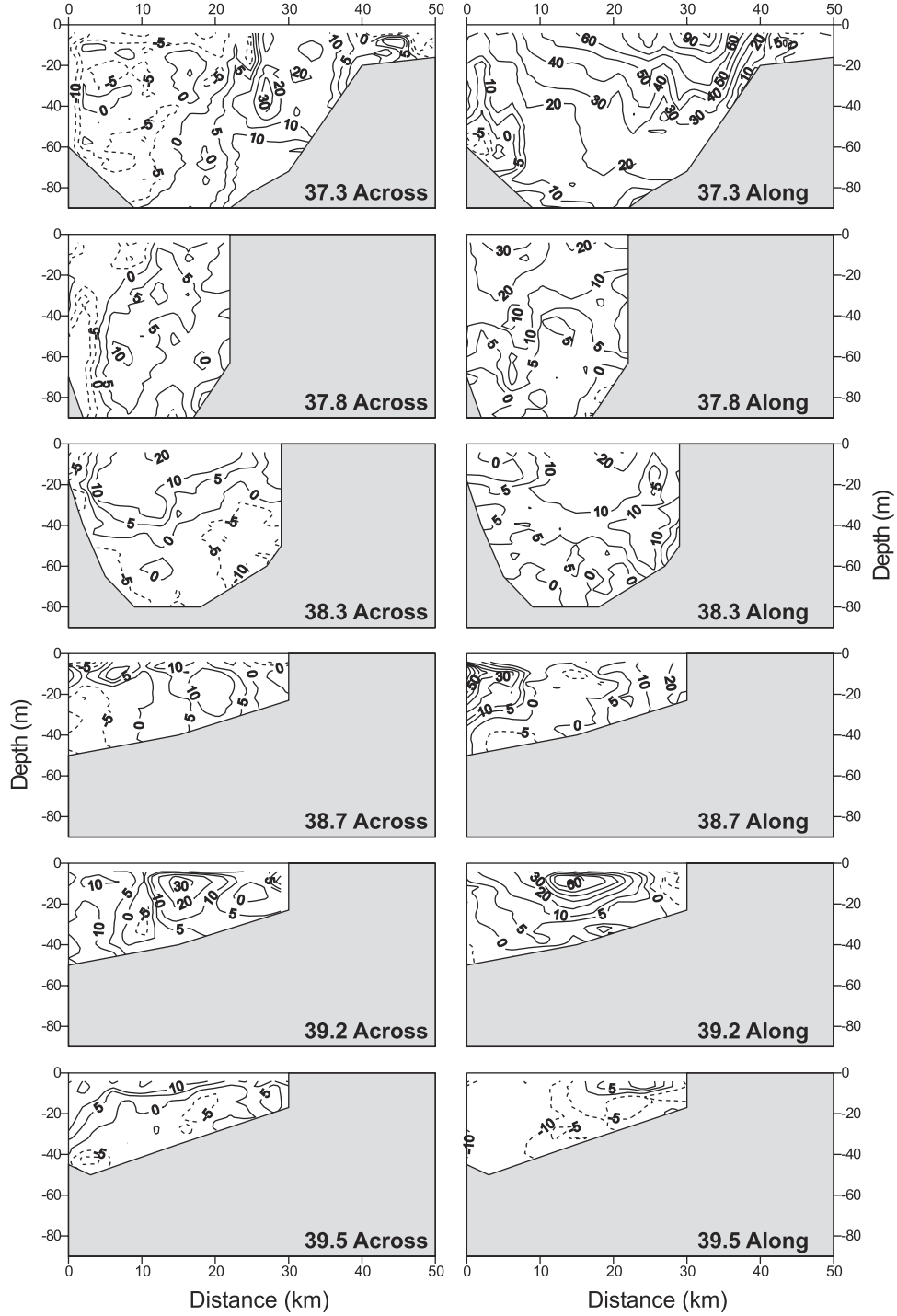

Figure 5. Vertical section of alongshore and across-shore currents (cm s^{-1}) along each NE trending cross-shelf track: between stations 2 and 3, 4 and 5, 6 and 7, 8 and 9, 10 and 11, and 12 and 13. The right panel is the alongshore (N-S) component, and the left panel is the across-shore (E-W) component. (Solid lines are positive velocities; dashed lines are negative velocities).

to the upwelling and cross-shelf intrusion process. Secondary thermoclines (stations 10 and 12) and mid-depth temperature and salinity inversions (stations 4 and 12) suggest complex interactions and mixing. Low-salinity surface layers were observed at stations 1, 3, and 5 off Valdivia, Toltén River, and Imperial River. The subsurface intrusion of higher-salinity water from offshore was noted at all stations (Figures 8c and 8d). Halocline strength mirrored the thermocline. Oxygen profiles (Figures 8e and 8f) clearly show the intrusion of low-O_2 ESSW into the coast. Below the surface, O_2 decreases at all stations except for minor inversions at stations 2, 4, and 12 at about 30 m. These distributions suggest that the onshore advection of low-oxygen water dominate processes such as air-sea gas exchange and vertical mixing in these coastal waters.

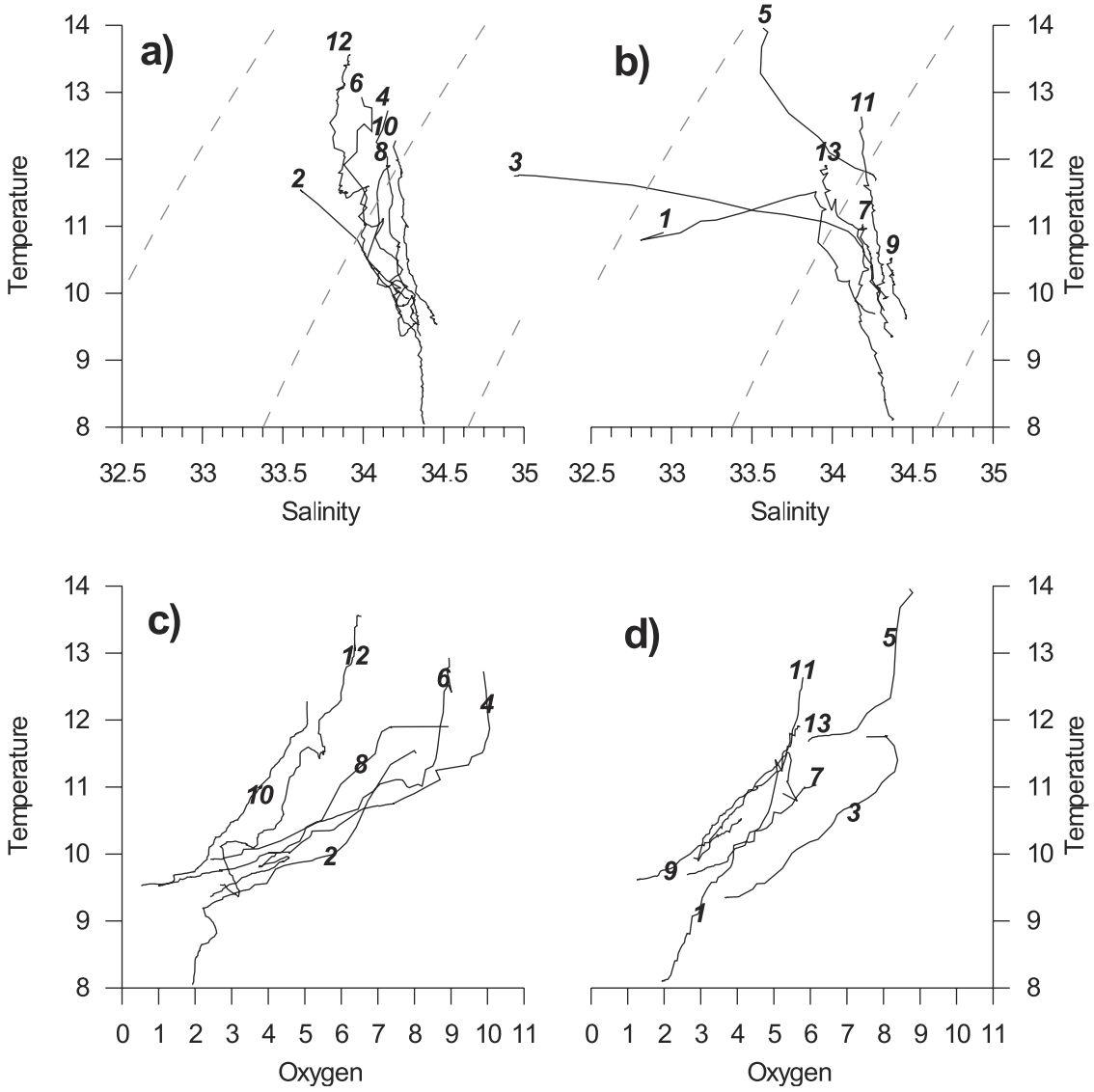

Figure 6. Temperature/salinity and temperature/O_2 plotted for each of the first 13 CTD stations. (a) and (c) Offshore section and (b) and (d) inshore section.

[33] The strong vertical oxygen gradients suggest a combination of cross-shelf flow and vertical advection. The layering was observed in O_2, temperature, and salinity at stations 2, 3, and 12, suggesting mixing and interleaving processes are present.

[34] To further illustrate the connection between the deeper waters and the surface, two sections were constructed: one consisting of the inshore stations from Valdivia to Lavapie Point and another consisting of offshore stations along the same route. (Figure 9 and Figure 10). The temperature section shows the subsurface intrusion of cold water into the inner shelf with more cold water present inshore than offshore, especially between 40° and 38.5°S. Subsurface salinity also shows the intrusion of salty water inshore. Since the subsurface water has low oxygen, its source is the undercurrent. Note how the surface expression of the upwelling is the low temperatures at 40° and 39°S, while the subsurface distributions show coldest bottom temperatures in the southern part of the region (nearer 40°S). The low-salinity and low-density surface water present in the surface layer in the southern region (where the Calle Calle, Toltén, and Imperial Rivers flow in) may provide enough buoyancy to keep a cap on the deeper upwelling water.

5. Discussion

[35] The observations made in December 1998 show a complex pattern of coastal upwelling combined with buoyancy inputs from coastal rivers. The upwelling is clearly affected by the capes (Lavapie Point) and platforms (inshore of Mocha Island). The extension of the cold surface waters north from Lavapie Point is very reminiscent of the plume extending southward across Monterey Bay [*Rosenfeld et al.*, 1994].

[36] In this section we discuss evidence for coastal currents, upwelling centers, residence time, and stratification in the context of our data and previous papers.

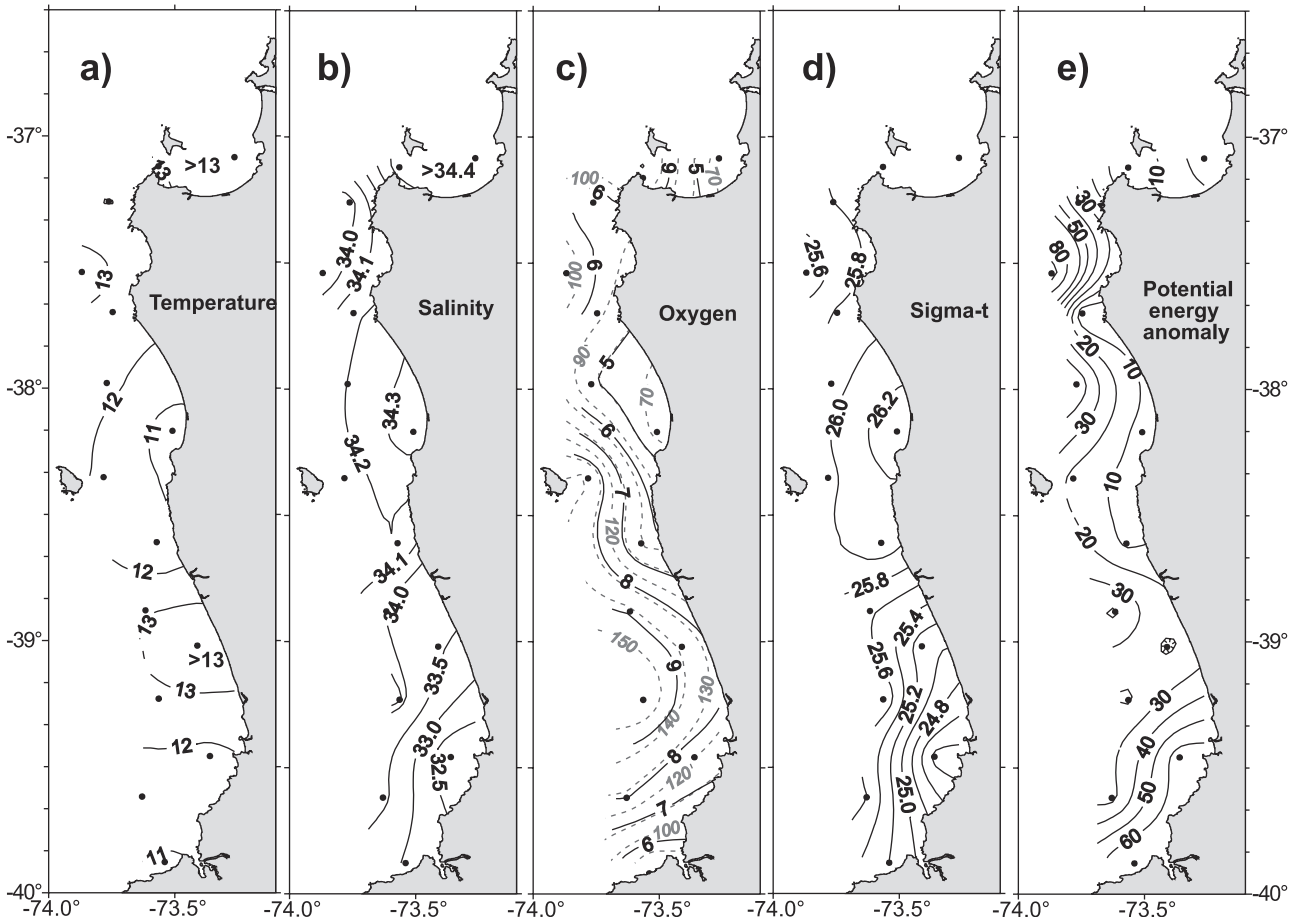

Figure 7. Surface maps of (a) temperature (°C), (b) salinity (practical salinity unit (psu)), (c) oxygen (mL L^{-1}), (d) density (sigma-*t*) (kg m^{-3}), and (e) stratification index (J m^{-3}).

[37] The river inflow in the southern part of the region should set up a southward flowing coastal current because of Coriolis acceleration. The geography of the coastline south of the Imperial River is relatively simple, and it is here that we expect to see a well-defined coastal current. The surface salinity distribution (Figure 7b) shows the presence of a buoyant plume, and the ADCP-measured currents (Figures 4 and 5) show southward currents off Imperial River and south of Toltén River. Off the Calle Calle River (Valdivia) no southward current was evident in the ADCP record. It is possible that the upwelling observed in the area causes a northward current overwhelming the effects of the buoyant plume, although tidal aliasing is certainly possible. The cross-shore density gradients in this region are ambiguous. While the surface density distribution suggests a southward current, examination of dynamic heights referenced to 20 or 30 m indicates a more complicated story. This is because high-density water intrudes beneath the buoyant surface layer. Thus, while the surface density distribution suggests a southward coastal current, the dynamic heights might suggest a northward baroclinic current. The sparse distribution of our CTD stations makes a more detailed analysis questionable. Nevertheless, we do have evidence for buoyant plumes south of the Imperial River. These buoyant plumes will no doubt create coastal currents that will contribute to the balance of forces in the region. The local coastal currents will vary depending on the strength and direction of the winds and the buoyant inflow. They should be stronger in the winter when rainfall is higher.

[38] Upwelling appears to occur all along this coast with significant variability. The SST and color images suggest a conceptual model of general upwelling along this part of the Chile coast. Overlaid on this are offshore and onshore advective features that move warm, low-chlorophyll water onshore or colder, high-chlorophyll water offshore. Warm, low-chlorophyll surface water is onshore at 39.9°, 39°, 38°, and 37.3°S. Cold, high-chlorophyll surface water is offshore at 39.2°, 38.6°, and 37.5°S. This distribution leads to alongshore scaling of about 80 km with respect to the mesoscale cross-shore advective features. These patterns are consistent with the analysis of *Cáceres and Arcos* [1991], who observed filaments to cluster around the submarine canyons north of Mocha Island and Santa Maria Island. If these features are truly semipermanent during upwelling conditions, they present an opportunity to study effects on larval distributions. Additional SST climatology would answer this question.

[39] The presence of upwelling, jets, filaments, and strong currents result in high across-shore currents relative to alongshore currents: Cross-shelf currents are often 1/10

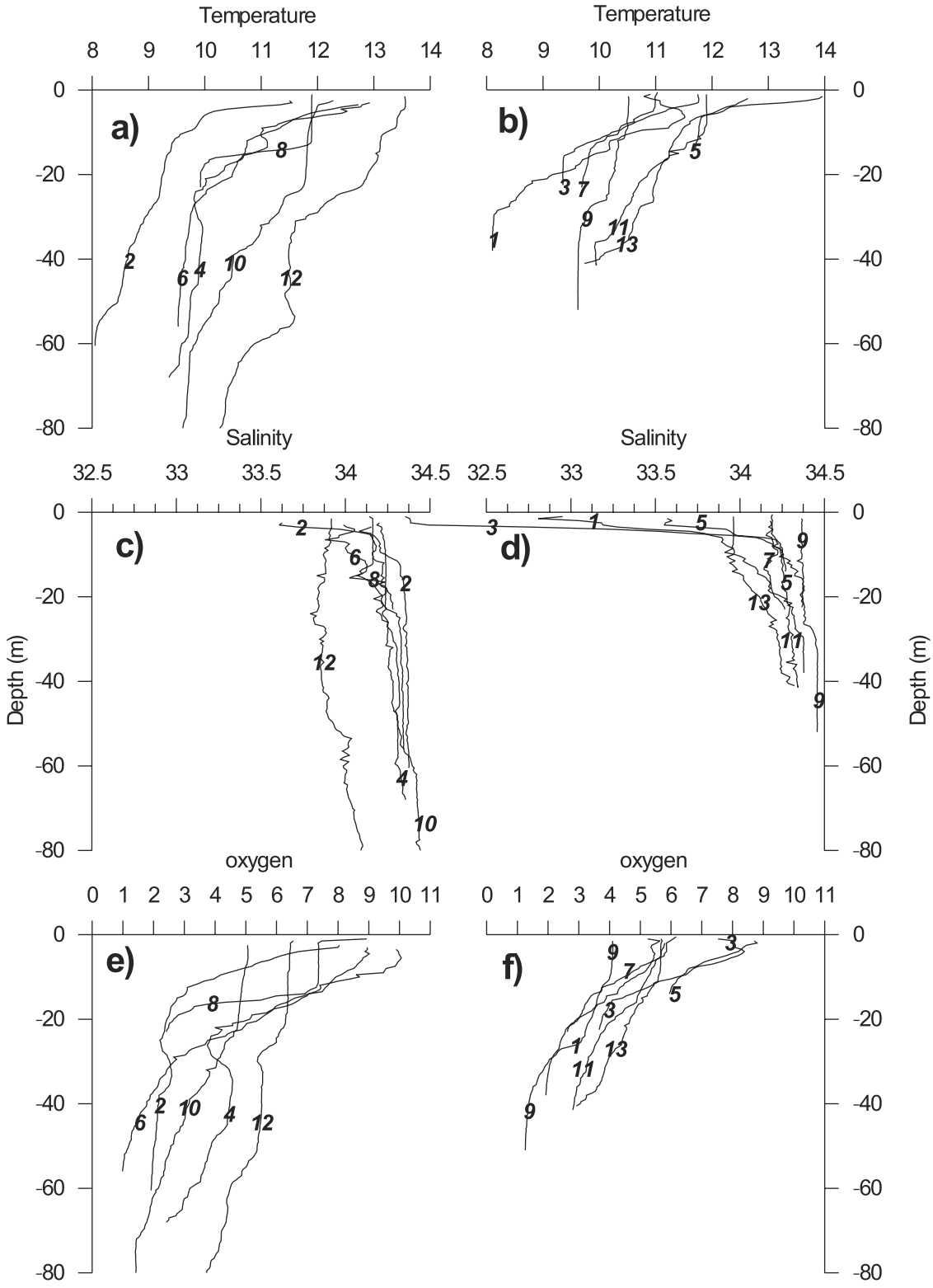

Figure 8. Temperature (°C), salinity (psu), and oxygen profiles (mL L^{-1}) at stations indicated. Inshore stations are on right, and offshore stations are on left.

the alongshore currents. In this region, across-shore currents are often 1/2 the alongshore currents. These values indicate the strong cross-shore transport that is occurring here. This process is most noticeable in the SeaWifs and SST images (Figure 4).

[40] The residence time of shelf waters is important if fisheries recruitment processes are to be understood. If we assume the circulation scale is about 60 km along this coast, the 0.5 m s^{-1} currents between 37 and 38°S would result in a residence time of about 1.5 days. Farther south the weaker

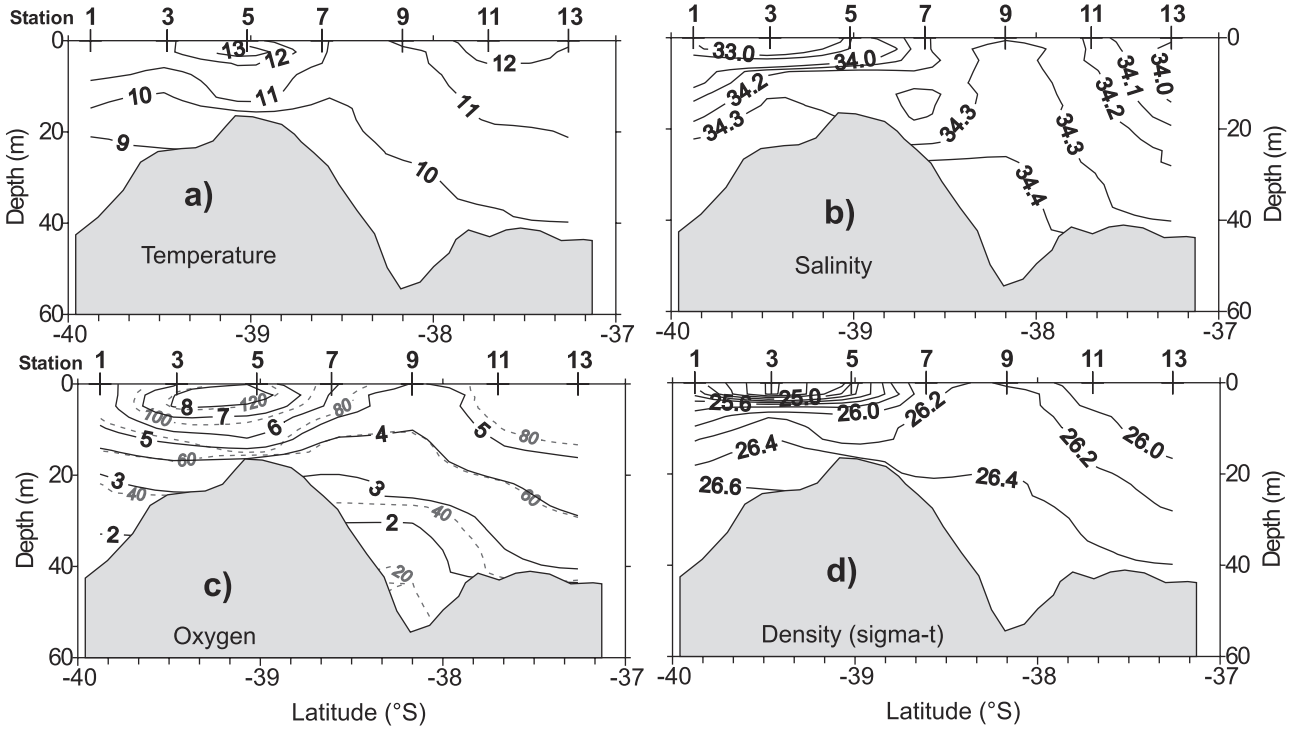

Figure 9. Alongshore vertical sections of (a) temperature (°C), (b) salinity (psu), (c) oxygen (mL L^{-1}) and percentage of saturation (dashed line), and (d) density (sigma-*t*) (kg m^{-3}). "Inshore" section refers to the stations nearest shore (1, 3, 5, . . ., 13).

currents (0.25 m s^{-1}) imply a residence time of 3 days. Deeper currents in both areas are weaker, yielding lower residence times. Overall, residence times in the area are probably less than 7 days.

[41] Stratification varied significantly as is typical of coastal upwelling systems. Stratification (Figure 7e) reached values of 20 to 70 J m^{-3}. Over a 2-day time period this stratification would require between 2.3 and 8.1 mW m^{-2} to achieve mixing (see *Atkinson and Blanton* [1986] for method). Since even strong winds provide less than 5 mW m^{-2}, the buoyancy influx apparently dominates the stratification: Normal upwelling winds (10–20 m s^{-1}) in the summer do not destroy the stratification created by the river runoff. The shallow area inshore of Mocha Island was relatively well mixed compared with areas north or south. Examination of the alongshore sections (Figure 10) indicates that the low-salinity surface layer caused higher stratification south of Mocha Island. North of Mocha Island, warm waters caused stratification. The warming was caused by insolation and by intrusions of warm water from offshore eddies. Apparently, wind and/or current mixing in the shallow waters behind Mocha Island were sufficient to eliminate stratification.

[42] The intensity of upwelling along this coast is no doubt related to both alongshore wind stress and topographic effects [*Figueroa and Moffat*, 2000]. Figure 3 of *Figueroa and Moffat* [2000] shows that while the wind stress component amounts to $1–2 \times 10^{-5}$ m s^{-1} with a peak near Punta Lavapie, the topographic component increased to a maximum of 3×10^{-5} m s^{-1} at that same location. To examine this further, the parameters specific to the area observed are used to make similar calculations. Vertical velocities depend on wind stress and topographic effects as follows:

$$w_s = \tau/(\rho\, fL)$$

$$w_t = \frac{Hv^2}{f\,S^2}\tan\,\alpha$$

The parameters are defined and typical values for the Lavapie point area are shown in Table 1. Using these values, the vertical velocity related to wind stress is 0.15×10^{-3} m s^{-1}. For comparison, using the equation given by *O'Brien* [1972] for two-layer ocean, the vertical velocity is $w_{s2} = \tau/\rho(g'H_1)^{1/2}$, where τ is the meridional wind stress, ρ is water density, g' is the reduced gravity, and H_1 is the depth of the first layer. With values from Table 1 the vertical velocity obtained is $w_{s2} = 0.2 \times 10^{-3}$m s^{-1}. Both values of vertical velocity are very close and similar to the determined off Nugurne Point (36°S) by *Kelly and Blanco* [1984].

[43] Local topography and/or coastline geometry have a great effect over alongshore current being able to induce or to modify the upwelling [*Arthur*, 1965; *Blanton et al.*, 1981; *Figueroa and Moffat*, 2000; *Rodrigues and Lorenzetti*, 2001]. Using values given in Table 1 and the meridional rate of change of coast orientation determined by *Figueroa and Moffat* [2000], the vertical velocity induced by topography is $w_t = 1.2 \times 10^{-3}$ m s^{-1}. This high value is due to the high meridional velocity of the current. In contrast, using the equation for conservation of vorticity [*Arthur*, 1965] with values given in Table 1, the vertical velocity induced by topography is 0.14×10^{-3} m s^{-1} for radii of

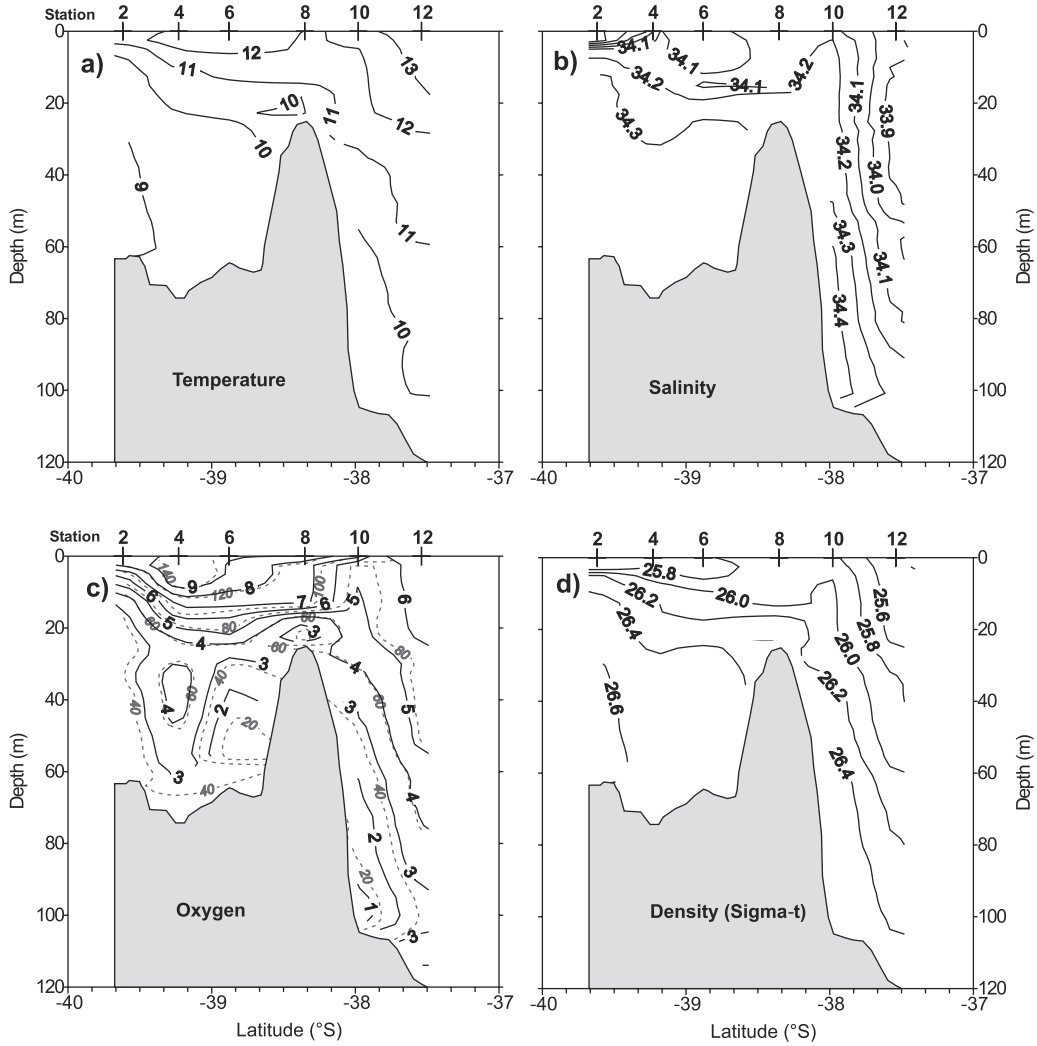

Figure 10. Alongshore vertical sections of (a) temperature (°C), (b) salinity (psu), (c) oxygen (mL L^{-1}) and percentage of saturation (dashed line), and (d) density (sigma-*t*) (kg m^{-3}). "Offshore" section refers to the outer stations (2, 4, 6, . . ., 12).

curvature as large as 60 km, a value very similar to the upwelling velocities related to wind stress.

[44] These results suggest that the high radii of curvature at points in our study area are enhancing the upwelling over and above what would be expected by normal coastal upwelling. It appears that the extreme changes in direction of isobaths at Lavapie Point lead to the very strong upwelling signature and northward currents we observed there. A final aspect of the flow here is the presence of an eddy feature offshore that even further enhances across-shore pressure gradients.

Table 1. Parameters for Calculating the Vertical Velocity

Parameter	Parameter	Value
Latitude	Φ	37°10′S
Coriolis parameter	f	-8.8×10^{-5}
Wind speed	W	10 m s^{-1}
Shelf width	L	10 km
Shelf depth	z	75 m
Current width	S	25 km
Meridional velocity	v	0.8 m s^{-1}
Water density of layer 1	ρ_1	1025.5 kg m^{-3}
Water density of Layer 2	ρ_2	1026.5 kg m^{-3}
Water density	ρ	1026.0 kg m^{-3}
Depth of layer 1	H_1	40 m
Depth of layer 2	H_2	80 m

6. Conclusions

[45] Our limited observations between Valdivia and Concepción during upwelling wind conditions suggest a coastal area strongly influenced by both local upwelling centers and the presence of offshore eddies. That, combined with the influx of runoff into some parts of the region and variations in heating and mixing, creates variations in stratification.

[46] This unique combination of forces and geography result in a complex physical oceanographic situation that apparently results in extremely high biological productivity. Regions such as this one are excellent examples of how carbon, fixed in a coastal upwelling system, is exported offshore. The highly productive fisheries suggest that much

of the primary production makes its way to higher trophic levels, but it eventually must be deposited in slope and trench sediments. Examination of those sediments might yield new insights into coastal upwelling and carbon sequestration processes.

[47] The similarities and differences between this region and the California upwelling regions are striking. It seems that comparative studies would be enlightening.

[48] **Acknowledgments.** We appreciate the funding support from the U.S. National Science Foundation (INT-96259334) and the Chilean National Fund for Advance Studies in Priority Areas (FONDAP). Universidad de Concepción, Old Dominion University. The Slover Endowment. Fundación Andes privided doctoral scholarship to Ricardo De Pol-Holz. Thanks to Andres Sepulveda and crew of the R/V *Kay Kay* for the contribution during the cruise. Data, imagery, and advice were provided by Frank Schwing and colleagues at NOAA, and the NASA SeaWifs project.

References

Arthur, R. S., On the calculation of vertical motion in eastern boundary currents from determinations of horizontal motion, *J. Geophys. Res.*, *70*, 2799–2803, 1965.

Atkinson, L. P., and J. O. Blanton, Processes that affect stratification in shelf waters with examples from the southeastern United States continental shelf, in *Baroclinic Processes on Continental Shelves, Coastal and Estuarine Ser.*, vol. 3, edited by C. N. K. Mooers, pp. 117–130, AGU, Washington, D. C., 1986.

Blanton, J. O., L. P. Atkinson, L. J. Piertrafesa, and T. N. Lee, The intrusion of Gulf Stream water across the continental shelf due to topographically-induced upwelling, *Deep Sea Res.*, *28*, 393–405, 1981.

Cáceres, M., Vórtices y filamentos observados en imágenes de satélite frente al área de surgencia de Talcahuano, Chile central, *Invest. Pesq. (Chile)*, *37*, 55–66, 1992.

Cáceres, M., and D. F. Arcos, Variabilidad en la estructura espacio-temporal de un area de surgencia frente a la costa de Concepción, Chile, *Invest. Pesq. (Chile)*, *36*, 27–38, 1991.

Davila, P. M., D. Figueroa, and E. Müller, Freshwater input into the coastal ocean and its relation on the salinity distribution off Austral Chile (35–54), paper presented at Sixth International Conference on Southern Hemisphere Meteorology and Oceanography, Am. Meteorol. Soc., Santiago, Chile, 2000.

Figueroa, D., and C. Moffat, On the influence of topography in the induction of coastal upwelling along the Chilean coast, *Geophys. Res. Lett.*, *27*, 3905–3908, 2000.

Gunther, E. R., A report on the oceanographical investigations in the Peru coastal current, *Discovery Rep.*, *13*, 107–276, 1936.

Kelly, R., and J. L. Blanco, Proceso de surgencia en Punta Nugurne, Chile (Lat. 36°S), marzo 1983, *Invest. Pesq.* (*Chile*), *31*, 89–94, 1984.

O'Brien, J., Models of coastal upwelling, paper presented at Symposium on Numerical Models of Ocean Circulation, Natl. Acad. of Sci., Washington, D. C., 1972.

Rodrigues, R., and J. Lorenzetti, A numerical study of the effects of bottom topography and coastline geometry on the southeast Brazilian coastal upwelling, *Cont. Shelf Res.*, *21*, 371–394, 2001.

Rosenfeld, L. K., F. B. Schwing, N. Garfield, and D. E. Tracy, Bifurcated flow from an upwelling center: A cold water source for Monterey Bay, *Cont. Shelf Res.*, *14*, 931–964, 1994.

Silva, N., and S. Neshyba, On the southernmost extension of the Peru-Chile Undercurrent, *Deep Sea Res., Part A*, *26*, 1387–1393, 1979.

Strub, P. T., J. M. Mesias, V. Montecino, J. Rutllant, and S. Salinas, Coastal ocean circulation off western South America, in *The Global Coastal Ocean—Regional Studies and Synthesis*, vol. 11, edited by A. R. Robinson and K. H. Brink, pp. 273–313, John Wiley, New York, 1998.

L. P. Atkinson, J. L. Blanco, and A. Valle-Levinson, Center for Coastal Physical Oceanography, Old Dominion University, 768 W 52nd Street, Norfolk, VA 23529, USA. (atkinson@ccpo.odu.edu)

R. De Pol-Holz, D. Figueroa, V. A. Gallardo, and W. Schneider, Departamento de Fisica de la Atmosfera y del Oceano, University of Concepción, Barrio Universitario S/N, Concepción, Chile. (ricardo@porfc.udec.cl; dfiguero@udec.cl; vagallar@udec.cl; wschnei@udec.cl)

M. Schmidt, SeaWIFS Project and SAIC, NASA/Goddard Space Flight Center, Greenbelt, MD 20771, USA. (mschmidt@gsfc.nasa.gov)

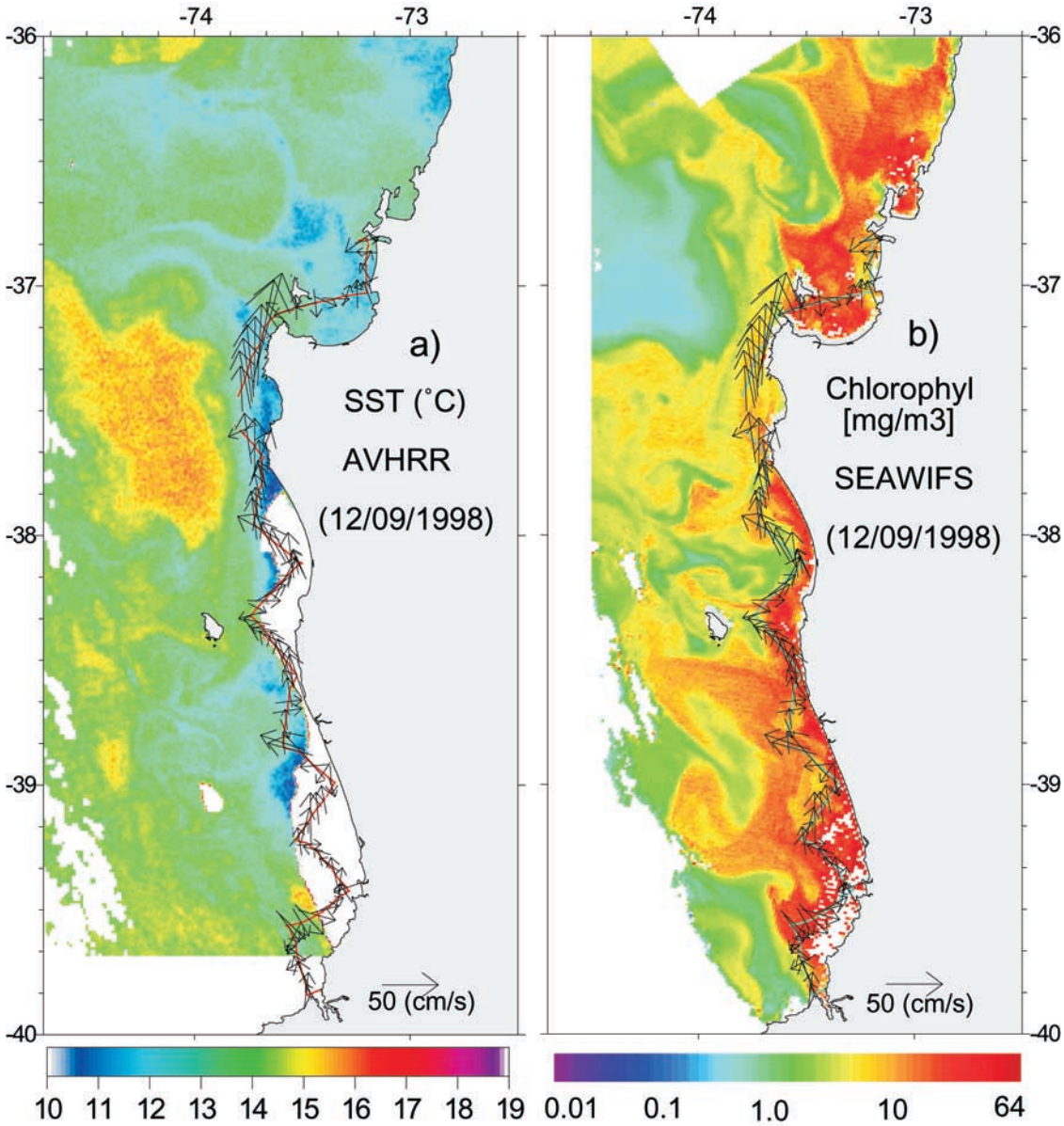

Figure 4. (a) Sea surface temperature from advanced very high resolution radiometer readings for 9 December 1998. (b) Surface chlorophyll SeaWifs image for 9 December 1998. Currents at 4 m depth, every fifth observation, are plotted. The 50 cm s^{-1} vector is indicated.